

# GDF-15 prevents LPS and D-galactosamine-induced inflammation and acute liver injury in mice

MIN LI<sup>1,2</sup>, KUI SONG<sup>3</sup>, XIAOWEN HUANG<sup>4</sup>, SIMAO FU<sup>4</sup> and QIYI ZENG<sup>1</sup>

<sup>1</sup>Department of Pediatrics, Zhujiang Hospital, Southern Medical University, Guangzhou, Guangdong 510515;

Departments of <sup>2</sup>Pharmacy and <sup>3</sup>Hematology, The First Affiliated Hospital of Jishou University,

Jishou, Hunan 416000; <sup>4</sup>Department of Pediatrics, Boai Hospital of Zhongshan

City, Zhongshan, Guangdong 528400, P.R. China

Received March 4, 2018; Accepted June 22, 2018

DOI: 10.3892/ijmm.2018.3747

**Abstract.** Growth differentiation factor-15 (GDF-15) is a transforming growth factor (TGF)- $\beta$  superfamily member with a poorly characterized biological activity, speculated to be implicated in several diseases. The present study aimed to determine whether GDF-15 participates in sepsis-induced acute liver injury in mice. Lipopolysaccharide (LPS) and D-galactosamine (D-GalN) were administered to mice to induce acute liver injury. Survival of mice, histological changes in liver tissue, and levels of inflammatory biomarkers in serum and liver tissue were evaluated following treatment with GDF-15. The underlying mechanism was investigated by western blotting, ELISA, flow cytometry, and reverse transcription-quantitative polymerase chain reaction using Kupffer cells. The results demonstrated that GDF-15 prevented LPS/D-GalN-induced death, increase in inflammatory cell infiltration and serum alanine aminotransferase and aspartate aminotransferase activities. In addition, GDF-15 treatment reduced the production of hepatic malondialdehyde and myeloperoxidase, and attenuated the increase of interleukin (IL)-6, tumor necrosis factor (TNF)- $\alpha$ , and IL-1 $\beta$  expression in serum and liver tissue, accompanied by inducible nitric oxide synthase (iNOS) inactivation in the liver. Similar changes in the expression of inflammatory cytokines, IL-6, TNF- $\alpha$  and IL-1 $\beta$ , and iNOS activation were observed in the Kupffer cells. Further mechanistic experiments revealed that GDF-15 effectively protected against LPS-induced nuclear factor (NF)- $\kappa$ B pathway activation by regulating TGF $\beta$ -activated kinase 1 (TAK1) phosphorylation in Kupffer cells. In conclusion, GDF-15 reduced the activation of pro-inflammatory

factors, and prevented LPS-induced liver injury, most likely by disrupting TAK1 phosphorylation, and consequently inhibiting the activation of the NF- $\kappa$ B pathway in the liver.

## Introduction

Sepsis, a systemic inflammatory the potential prevention role of GDF-15 in sepsis, mice were intravenously injected with GDF-15 (10 mg/kg) after being administered with LPS (20 mg/kg) and D-GalN (700 mg/kg). Mice in the negative control group were treated with vehicle (sterile PBS). All of the mice were monitored for 36 h to assess their survival rates response syndrome caused by severe microbial infection, remains the leading cause of death in intensive care units worldwide (1,2). Research efforts in the field of sepsis have focused primarily on the innate immune system, and typically, have conceptually viewed sepsis as a hyper-inflammation syndrome (3,4). Acute liver injury, characterized by severe hepatic injury with failure of hepatocyte function, is an important cause of morbidity and mortality in patients with sepsis (5). The importance of macrophage activation and endotoxin-mediated proinflammatory cytokine production during liver injury is evident from numerous models of acute and chronic liver diseases (6). Pro-inflammatory cytokines, such as tumor necrosis factor (TNF)- $\alpha$ , interleukin (IL)-6, and IL-1, are primarily involved in the promotion of inflammatory processes, and have an important role in liver injury (7,8).

Lipopolysaccharide (LPS), a constituent of the outer cell wall of gram-negative bacteria, has the ability to elicit a severe inflammatory response in organisms, ultimately resulting in systemic inflammatory response syndrome. Liver cells, including Kupffer cells, hepatocytes and sinusoidal endothelial cells, can take up circulating LPS, following both *ex vivo* exposure to LPS and LPS injection (9). D-galactosamine (D-GalN) can increase the sensitivity of liver cells to LPS, and induce liver injury, as well as elevate serum TNF- $\alpha$  levels abnormally in the presence of low-dose LPS (10). Therefore, the combined use of LPS and D-GalN is used to establish a successful liver dysfunction model (10).

Growth differentiation factor-15 (GDF-15), also known as macrophage inhibitory cytokine-1 (MIC-1) and nonsteroidal anti-inflammatory drug-activated gene-1 (NAG-1), is a

---

*Correspondence to:* Dr Qiyi Zeng, Department of Pediatrics, Zhujiang Hospital, Southern Medical University, 253 Industrial Avenue, Guangzhou, Guangdong 510515, P.R. China  
E-mail: ZQY\_88@163.com

**Key words:** sepsis, acute liver injury, growth differentiation factor-15, transforming growth factor  $\beta$ -activated kinase 1, nuclear factor- $\kappa$ B

divergent member of the transforming growth factor (TGF)  $\beta$  family related to immunosuppression, anti-apoptosis, anti-inflammation, growth inhibition, and cancer cell invasion (11). Previous investigations have suggested that GDF-15 has important roles in heart diseases. In patients with atrial fibrillation, GDF-15 is an independent risk indicator for major bleeding and all-cause mortality, although not for stroke (12). In patients with acute heart failure, enrolled in the RELAX in Acute Heart Failure study, increases in GDF-15 levels, although not baseline measurements, were related to a greater risk of adverse outcomes (13). A previous experimental study has demonstrated that GDF-15 deficiency augments inflammatory responses, and exacerbates LPS-induced renal and cardiac injury, while GDF-15 overexpression protects the kidney and heart from LPS-induced organ dysfunction (14). The present study aimed to determine whether GDF-15 participates in sepsis-induced acute liver injury in mice, by establishing an experimental model for acute liver injury using LPS and D-GalN. The histological changes, inflammation status, and potential mechanism were investigated.

## Materials and methods

**Animals and experimental models.** C57BL/6 male mice (5–6 weeks old, 20–22 g weight) were obtained from Beijing HFK Bioscience Co., Ltd. (Beijing, China). The animals were housed on 12-h light/dark cycles at 25°C. Animals received standard animal rodent chow and water *ad libitum*. Care of animals and the experimental protocols for this study were approved by the Institutional Animal Use Committee of the Southern Medical University (Guangzhou, China).

LPS (*Escherichia coli* 0111:B4), D-GalN and curcumin were obtained from Sigma-Aldrich (Merck KGaA, Darmstadt, Germany). Acute liver injury was induced by intraperitoneal injection of 20  $\mu$ g/kg body weight of LPS and 700 mg/kg body weight of D-GalN. A total of 48 mice were randomly divided into 3 groups. Mice in the control group received injections of PBS alone. Mice in the model group received LPS injections and 15 min later were injected with D-GalN. Mice in the GDF-15 treatment group were injected intravenously with GDF-15 [1 mg/kg body weight (15); purchased from Sino Bio, Beijing, China] 10 min after the D-GalN injection. A total of 6 mice in each group were anesthetized and sacrificed 6 h following LPS injection. The liver tissue and blood serum were collected for further analysis. A total of 10 mice in each group were used for survival analysis for an additional 36 h.

**Measurement of serum aminotransferase activities.** Serum aspartate aminotransferase (AST) and alanine aminotransferase (ALT) activities were measured via the enzymatic kinetic method, by using an automatic biochemistry analyzer (SELECTA XL; Vital Scientific, Dieren, Netherlands) according to the manufacturers' protocol.

**Histological analysis.** Liver tissues were fixed in 4% paraformaldehyde solution at room temperature (22–25°C) for 48 h, embedded in paraffin, and sectioned at 5- $\mu$ m. Following dehydration, sections were stained with hematoxylin and eosin (H&E) at room temperature (22–25°C) according to the previously reported methods (hematoxylin staining for 3 min

and eosin staining for 1 min) (16). Grading was adapted from t'Hart *et al* (17) and described as: 1, normal rectangular structure; 2, rounded hepatocytes with an increase in the sinusoidal spaces; 3, vacuolization; 4, nuclear picnosis; and 5, necrosis. Histological evaluations of the damage scores were performed in a blinded manner by 3 different observers.

**ELISA.** The IL-6 (cat. no. EMC004.96; NBS Biologicals, Ltd., Shenzhen, China; <http://www.nbs-bio.com/>), TNF- $\alpha$  (cat. no. EMC102a.96; NBS Biologicals, Ltd.), IL-1 $\beta$  (cat. no. EMC001b.96; NBS Biologicals, Ltd.), cyclooxygenase-2 (COX-2; cat. no. ab210574; Abcam, Cambridge, UK) and monocyte chemoattractant protein-1 (MCP-1; cat. no. EMC113.96; NBS Biologicals, Ltd.) levels in the serum, liver tissues and medium were determined by ELISA analysis, following the instructions of the kit manufacturer.

**Measurement of malondialdehyde (MDA).** MDA was quantified as thiobarbituric acid reactive substances (TBARS), according to previously published methods (18). Briefly, the weighed samples were homogenized in 1 ml 5% trichloroacetic acid. The samples were centrifuged (10,000  $\times$  g) at 4°C for 5 min and 250  $\mu$ l of the supernatant was reacted with the same volume of 20 mM thiobarbituric acid for 35 min at 95°C, followed by 10 min at 4°C. Sample fluorescence was measured using a spectrophotometric plate reader at the wavelength of 545 nm.

**Liver myeloperoxidase (MPO) assay.** The liver MPO was determined as previously described (19). Briefly, the liver tissue was homogenized (50 mg/ml) in 0.5% hexadecyltrimethylammonium bromide in 10 mM 3-(N-morpholino) propanesulfonic acid and centrifuged (15,000  $\times$  g) at 4°C for 40 min. The suspension was then sonicated 3 times for 30 sec at 1 min intervals. An aliquot of supernatant was mixed with a solution of 1.6 mM tetramethylbenzidine and 1 mM H<sub>2</sub>O<sub>2</sub>. The activity was measured spectrophotometrically as the change in absorbance at 37°C with a microplate reader (Thermo Fisher Scientific, Inc., Waltham, MA, USA). The results are expressed as units of MPO activity per gram of protein, as determined by the Bradford assay (Beyotime Institute of Biotechnology, Beijing, China).

**Immunofluorescence staining.** Liver tissues were fixed in 4% paraformaldehyde solution at room temperature (22–25°C) for 48 h, embedded in paraffin, and sectioned at 5- $\mu$ m. Following dehydration and antigen retrieval (3 min under high pressure), tissue samples were blocked with goat serum at room temperature (22–25°C) for 15 min and incubated with specific rabbit monoclonal antibody against inducible nitric oxide synthase (iNOS; 1:200; cat. no. ab15323; Abcam, Cambridge, UK) and rabbit monoclonal antibodies against CD68 (1:150; cat. no. ab125212; Abcam) at 4°C overnight. A secondary antibody, either fluorescein isothiocyanate (FITC; 1:100; cat. no. sc-2012) or cyanine (Cy) 3 (1:100; cat. no. sc-2010)-conjugated anti-rabbit or anti-mouse IgG (Santa Cruz Biotechnology, Inc., Dallas, TX, USA) was then added and incubated at 37°C for 1 h. The nuclei were stained with DAPI (Beyotime Institute of Biotechnology). Images were captured with a Nikon DX500 fluorescent laser-scanning microscope (Nikon Corporation, Tokyo, Japan).

**Cell culture and treatment.** Kupffer cells were obtained from Jennio Bio (Guangzhou, China), and they were confirmed by a short tandem repeat analysis. The cells were routinely maintained in DMEM (Invitrogen; Thermo Fisher Scientific, Inc.) with 10% fetal bovine serum (FBS; Merck KGaA) and 1% antibiotic-antimitotic reagent (Invitrogen; Thermo Fisher Scientific, Inc.). For treatments, Kupffer cells were plated in 6-well plates at  $2 \times 10^5$  per well. A total of 24 h post-plating, LPS (2  $\mu\text{g/ml}$ ) was added to the cells, while sterile PBS was used as negative control. GDF-15 (10 ng/ml) was added into the supernatant of LPS-treated cells, as previous described (20). At 24 h post-treatment, the supernatant and total protein were collected for ELISA and western blotting analyses.

**Western blotting analysis.** Cells were collected and lysed with RIPA lysis buffer (Beyotime Institute of Biotechnology) containing 1/100 protease inhibitor cocktail (Merck KGaA). Following centrifugation at  $12,000 \times g$ ,  $4^\circ\text{C}$  for 15 min, the proteins were collected and used for concentration measurement with a BCA kit (Beyotime Institute of Biotechnology). Total protein (20  $\mu\text{g}$ ) from each sample was separated by SDS-PAGE (8 or 10%) and transferred to polyvinylidene fluoride membranes (Merck KGaA) electrophoretically. The membranes were blocked with 5% nonfat milk in Tris-buffered saline containing 0.5% Tween-20 and then incubated overnight at  $4^\circ\text{C}$  with the following primary antibodies from Cell Signaling Technology, Inc. (Danvers, MA, USA): nuclear factor (NF)- $\kappa\text{B}$  p65 (1:800; cat. no. 8242), phosphorylated (p)-TGF $\beta$ -activated kinase 1 (TAK1; 1:1,200; cat. no. 4505), TAK1 (1:800; cat. no. 9339), NF- $\kappa\text{B}$  p50 (1:1,000; cat. no. 12540), p-NF- $\kappa\text{B}$  inhibitor  $\alpha$  (I $\kappa\text{B}\alpha$ ; 1:800; cat. no. 5209), I $\kappa\text{B}\alpha$  (1:1,000; cat. no. 4814) and GAPDH (1:2,000; cat. no. 2118). The membranes were then incubated with horseradish-peroxidase conjugated anti-mouse (1:5,000; cat. no. ZDR5307) and anti-rabbit IgG (1:5,000; cat. no. ZDR5306; both from Zhongshan Golden Bridge Biotechnology Co., Ltd., Beijing, China), for 1 h at room temperature. The protein bands were developed using enhanced chemiluminescence detection reagent (Merck KGaA) and quantified using ImageJ (v1.8.0\_112; National Institutes of Health, Bethesda, MD, USA) (21). The relative expression was normalized to GAPDH levels.

**Flow cytometry.** Cultured Kupffer cells were collected and stained with unlabeled antibodies targeting iNOS (1:200; cat. no. ab15323; Abcam) in PBS for 1 h at room temperature. After washing with PBS 3 times, a secondary FITC-conjugated anti-rabbit antibody (1:500; cat. no. sc-2012; Santa Cruz Biotechnology, Inc.) was added for further incubation at  $4^\circ\text{C}$  for 1 h in dark. The cells were analyzed by flow cytometry on a BD FACSCalibur instrument. Data were analyzed using FlowJo software (v10.2; FlowJo, LLC, Ashland, OR, USA).

**Reverse transcription-quantitative polymerase chain reaction (RT-qPCR) analysis.** Total mRNA was extracted from the cells using TRIzol (Thermo Fisher Scientific, Inc.). Reverse transcription was performed following the protocol of the PrimeScript RT reagent kit with gDNA eraser (cat. no. RR047A; Takara Biotechnology Co., Ltd., Dalian, China). The Permix Taq kit (cat. no. RR066A; Takara Biotechnology Co., Ltd.)

was used for qPCR. All of the reactions were performed using the CFX96 Touch Real-Time PCR detection system (Bio-Rad Laboratories, Inc., Hercules, CA, USA). The qPCR conditions were as follows: Denaturation at  $94^\circ\text{C}$  for 2 min, amplification for 30 cycles at  $94^\circ\text{C}$  for 0.5 min, annealing at  $60^\circ\text{C}$  for 0.5 min and extension at  $72^\circ\text{C}$  for 1 min, followed by a terminal elongation step at  $72^\circ\text{C}$  for 10 min. The threshold cycle (Cq) values were determined by plotting the observed fluorescence against the cycle number. Cq values were analyzed using the comparative threshold cycle method and normalized to those of GAPDH (22). The relative gene expression levels were estimated using the following formula: Relative expression =  $2^{-[\text{Cq}(\text{iNOS}) - \text{Cq}(\text{GAPDH})]}$ . The sequence of primers for iNOS: Forward, 5'-GAGCGAGTTGTGGATTGTC-3' and reverse, 5'-CTCCTTTGAGCCCTTTTGT-3'; for GAPDH: Forward, 5'-GGTCGGAGTCAACGGATTGGTCG-3' and reverse, 5'-CCTCCGACGCCTGCTTACCAC-3'.

**Statistical analysis.** Data were expressed as means  $\pm$  standard deviation. All of the data were analyzed with SPSS 17.0 version (SPSS, Inc., Chicago, IL, USA). One-way analysis of variance followed by a Dunnett's post hoc test for multiple comparisons and a students' t test was used to compare two groups.  $P < 0.05$  was considered to indicate a statistically significant difference. Three to five random experiments were repeated.

## Results

**Protective effect of GDF-15 in LPS/D-GalN-induced acute liver injury.** To evaluate. As illustrated in Fig. 1A, LPS/D-GalN administration resulted in death in 80% of the mice death at 36 h compared with the PBS injection group. However, GDF-15 treatment efficiently enhanced the survival of mice (only 3 out of 10 mice were dead at 36 h post LPS/D-GalN injection; Fig. 1A). At 6 h post LPS/D-GalN injection, liver tissues from the mice were used for histological examination. Results from H&E staining identified hepatocyte necrosis and inflammatory cell infiltration in the model group (LPS/D-GalN administration alone), while these effects were markedly less evident in the GDF-15 treatment group (Fig. 1B). To determine the effect of GDF-15 on liver injury induced by LPS/GalN, the serum levels of AST and ALT were assessed. The levels of ALT and AST were significantly increased by LPS/D-GalN administration (Fig. 1C and D). However, GDF-15 treatment significantly decreased the activities of ALT and AST, compared with the model group (Fig. 1C and D). Collectively, these results demonstrated the preventative role of GDF-15 in LPS/D-GalN-induced acute liver injury.

**GDF-15 represses liver inflammation induced by LPS/D-GalN.** Subsequently, to determine the potential anti-inflammatory effect of GDF-15, the levels of the pro-MDA and MPO were monitored in liver. As presented in Fig. 2A, LPS/D-GalN administration increased the amount of MDA compared with the control group. However, compared with the model group, the content of MDA was decreased in the GDF-15-treated mice (Fig. 2A). In addition, an MPO assay demonstrated that GDF-15 dramatically attenuated LPS/D-GalN-induced leukocyte infiltration in liver (Fig. 2B). ELISA analysis



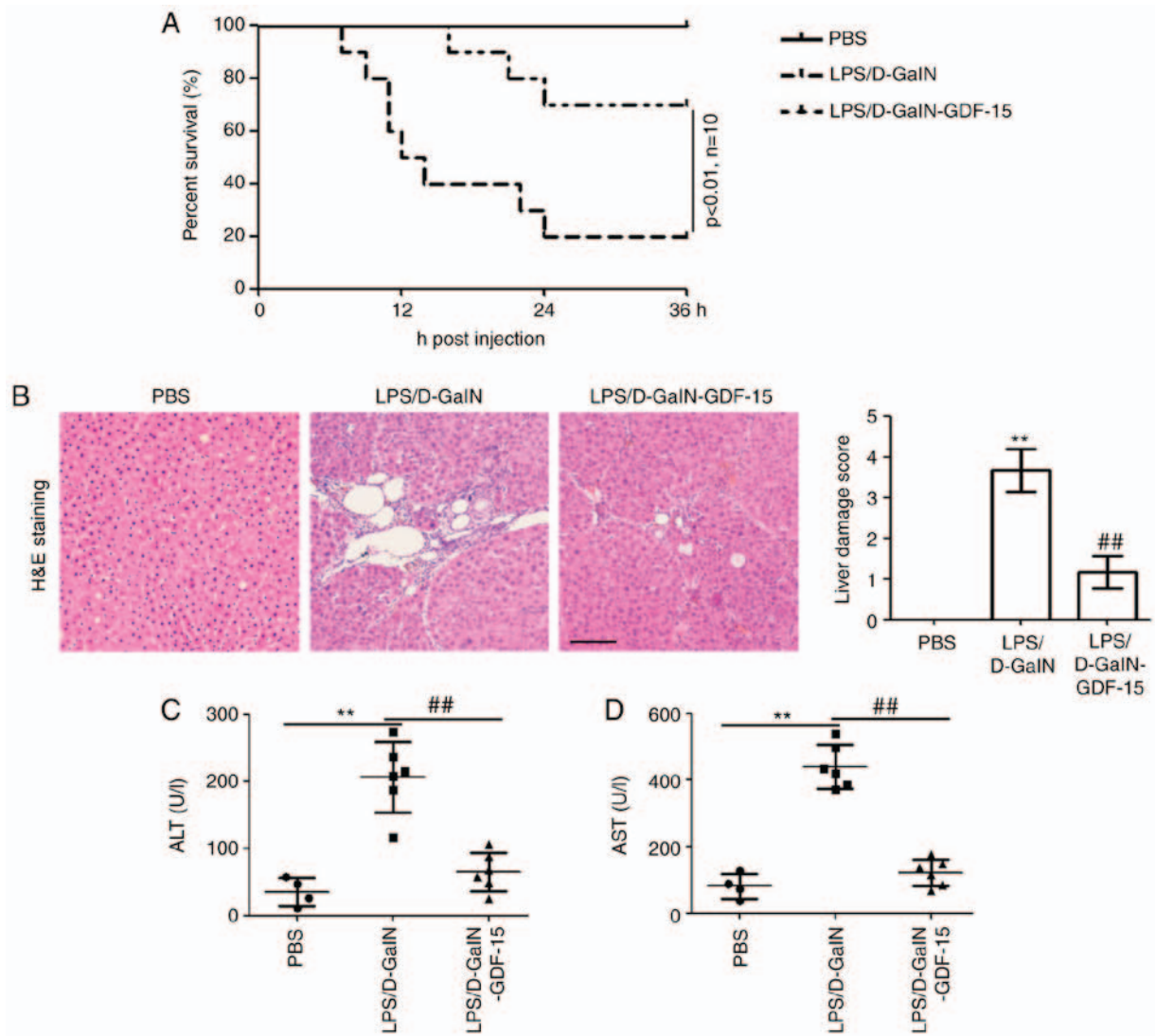


Figure 1. Protective effect of GDF-15 in acute LPS/D-GalN-induced liver injury. (A) Survival analysis was recorded for each group over 36 h, for each group (n=10 mice per group). (B) Representative images from H&E staining of liver tissue sections from each group (scale bar, 200  $\mu$ m). The liver damage score was quantified (n=6 mice per group). (C) Serum levels of ALT and (D) AST were determined (n=6 mice per group). \*\*P<0.01 compared with PBS group; ##P<0.01 compared with LPS/D-GalN group. GDF-15, growth differentiation factor-15; LPS, lipopolysaccharide; D-GalN, D-galactosamine; H&E, hematoxylin and eosin; ALT, alanine aminotransferase; AST, aspartate aminotransferase.

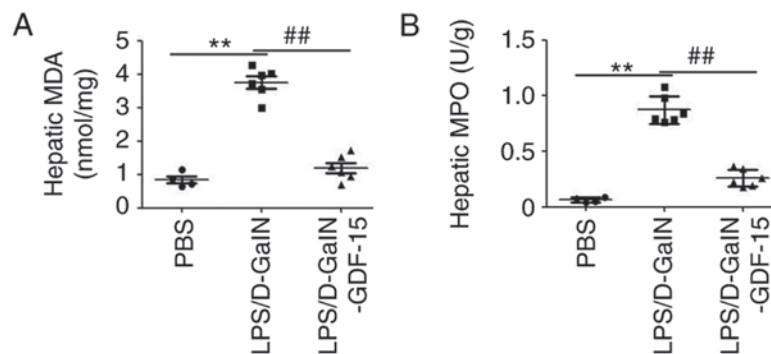


Figure 2. GDF-15 represses the activity of MDA and MPO induced by LPS/D-GalN. (A) The contents of MDA in liver samples were evaluated at 8 h following LPS/D-GalN administration. (B) An MPO kit was used to evaluate leukocyte infiltration in livers at 8 h following LPS/D-GalN administration. \*\*P<0.01 compared with PBS group; ##P<0.01 compared with LPS/D-GalN group (n=6). GDF-15, growth differentiation factor-15; MDA, malondialdehyde; MPO, myeloperoxidase; LPS, lipopolysaccharide; D-GalN, D-galactosamine.

demonstrated the upregulation of pro-inflammatory cytokines IL-6, TNF- $\alpha$  and IL-1 $\beta$  both in serum and liver tissue

of mice following LPS/D-GalN administration (Fig. 3). Furthermore, this increase in serum and hepatic IL-6, TNF- $\alpha$

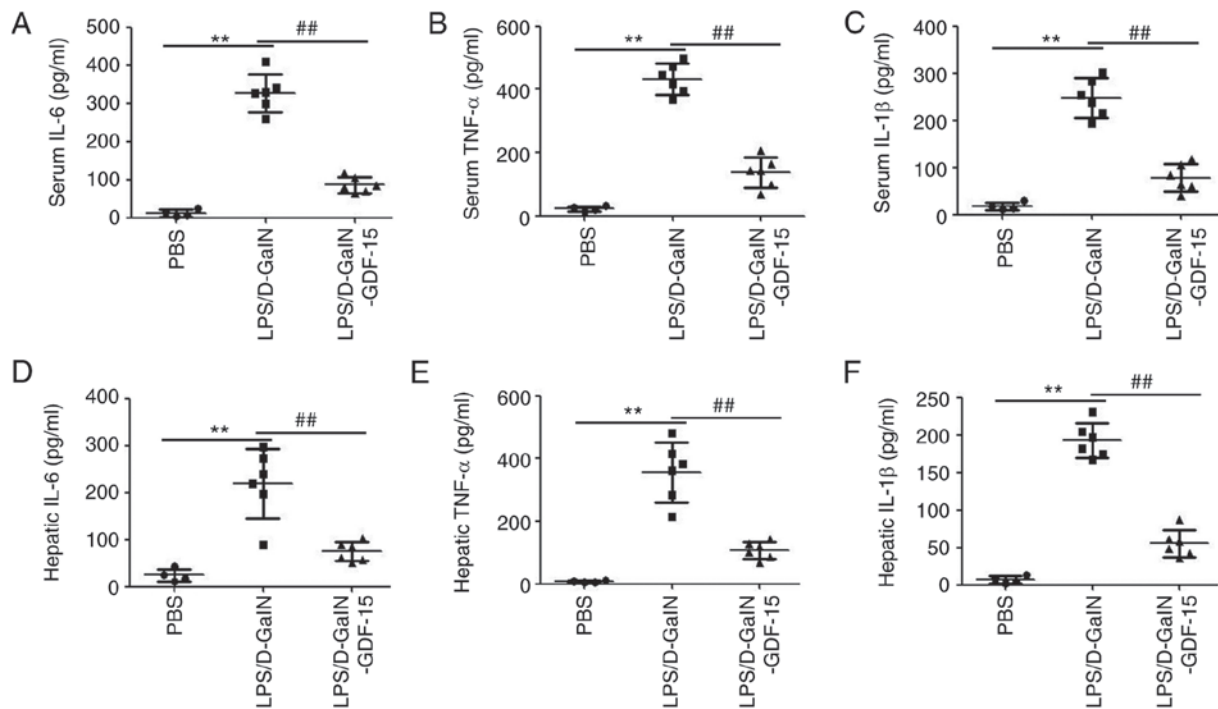


Figure 3. GDF-15 represses pro-inflammatory cytokine expression by LPS/D-GalN. (A) Serum levels of IL-6, (B) TNF-α and (C) IL-1β were evaluated by ELISA. (D) Hepatic levels of IL-6, (E) TNF-α and (F) IL-1β in livers were evaluated by ELISA. \*\*P<0.01 compared with PBS group; ##P<0.01 compared with LPS/D-GalN group (n=6). GDF-15, growth differentiation factor-15; LPS, lipopolysaccharide; D-GalN, D-galactosamine; IL, interleukin; TNF, tumor necrosis factor.

and IL-1β expression was prevented in mice treated with GDF-15 (Fig. 3). These results indicated that GDF-15 had an obvious anti-inflammatory activity *in vivo*.

**GDF-15 inhibits LPS/D-GalN-induced iNOS activation in liver.** To determine the effect of GDF-15 on macrophage activation, immunofluorescent staining was performed to detect iNOS-positive macrophages in liver tissue. Immunofluorescent staining of liver samples revealed that iNOS expression colocalizing with CD68, a macrophage marker, was markedly increased following LPS/D-GalN administration compared with the control group (Fig. 4A). However, compared with the model group, less iNOS/CD68-positive macrophages were observed in the GDF-15-treated mice (Fig. 4A). Then, the levels of the macrophage-associated pro-inflammatory cytokines COX-2 and MCP-1 were determined. The results demonstrated the increased expression of hepatic COX-2 and MCP-1 in mice following LPS/D-GalN administration (Fig. 4B and C). Treatment with GDF-15, however, inhibited the LPS/D-GalN-induced COX-2 and MCP-1 expression in liver (Fig. 4B and C). Collectively, these results suggested that GDF-15 inhibited the activation of pro-inflammatory macrophages *in vivo*.

**GDF-15 attenuates LPS-induced inflammation and iNOS activation in Kupffer cells.** To investigate the anti-inflammatory mechanism of GDF-15 in LPS/D-GalN-induced acute liver injury, GDF-15 was used to treat Kupffer cells *in vitro*. ELISA analysis was performed to determine the IL-6, TNF-α and IL-1β expression in the supernatant of the treated Kupffer cells. As presented in Fig. 5A-C, treatment of Kupffer cells

with LPS (2 μg/ml) significantly increased the levels of the pro-inflammatory cytokines IL-6, TNF-α and IL-1β, while GDF-15 treatment significantly inhibited this effect. Flow cytometry analysis indicated that LPS promoted the activation of pro-inflammatory Kupffer cells (measured as the % of iNOS-positive cells; Fig. 5D). However, the LPS-induced activation of pro-inflammatory Kupffer cells was significantly suppressed by GDF-15 treatment (Fig. 5D). RT-qPCR analysis also confirmed the inhibiting effect of GDF-15 on LPS-induced iNOS upregulation at the mRNA level (Fig. 5E). Finally, LPS administration upregulated the levels of macrophage-associated pro-inflammatory cytokines, COX-2 and MCP-1, in the supernatant of Kupffer cells, and this effect was significantly attenuated by GDF-15 treatment (Fig. 5F and G). These results indicated that GDF-15 attenuated LPS-induced inflammation and iNOS activation in Kupffer cells.

**GDF-15 protects against LPS-induced NF-κB pathway activation through regulating TAK1 phosphorylation in Kupffer cells.** To further investigate the anti-inflammatory mechanism of GDF-15 in Kupffer cells, western blotting analysis was performed to detect NF-κB p65, p-TAK1, TAK, NF-κB p50, p-IκBα and IκBα expression in Kupffer cells following LPS and GDF-15 treatment. As presented in Fig. 6A, NF-κB p65 expression was induced by LPS, compared with the negative control group (PBS). However, GDF-15 dramatically impaired the upregulation of NF-κB p65 (Fig. 6A), compared with the LPS group. GDF-15 also efficiently prevented the activation of TAK1 (Fig. 6B), which has been demonstrated to be the direct binding receptor of GDF-15 in macrophages (23). Furthermore, NF-κB p50 expression and phosphorylation of

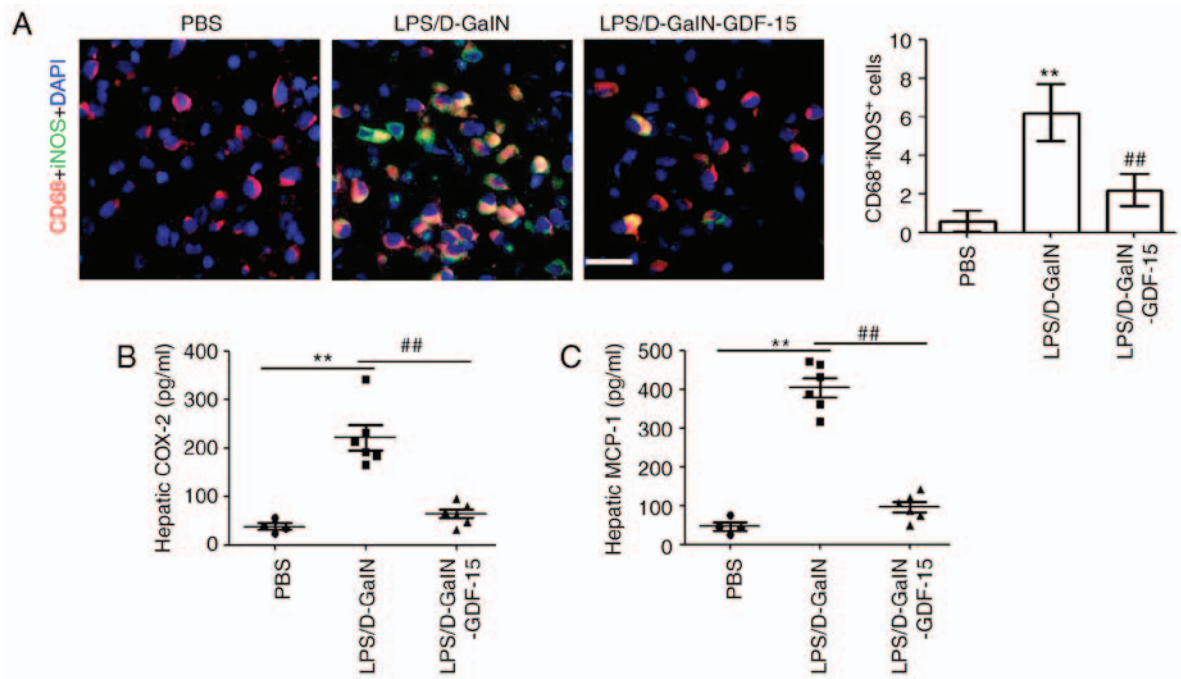


Figure 4. GDF-15 inhibits LPS/D-GalN-induced iNOS activation. (A) CD68 and iNOS positive cells in liver tissues were determined by immunofluorescent staining. Representative images and quantification of the % of CD68/iNOS-positive cells are shown (scale bar, 50  $\mu$ m). (B) The expression of COX-2 and (C) MCP-1 in livers was evaluated by ELISA. \*\* $P < 0.01$  compared with PBS group; ## $P < 0.01$  compared with LPS/D-GalN group ( $n = 3$ ). GDF-15, growth differentiation factor-15; LPS, lipopolysaccharide; D-GalN, D-galactosamine; iNOS, inducible nitric oxide synthase; COX-2, cyclooxygenase-2; MCP-1, monocyte chemoattractant protein-1.

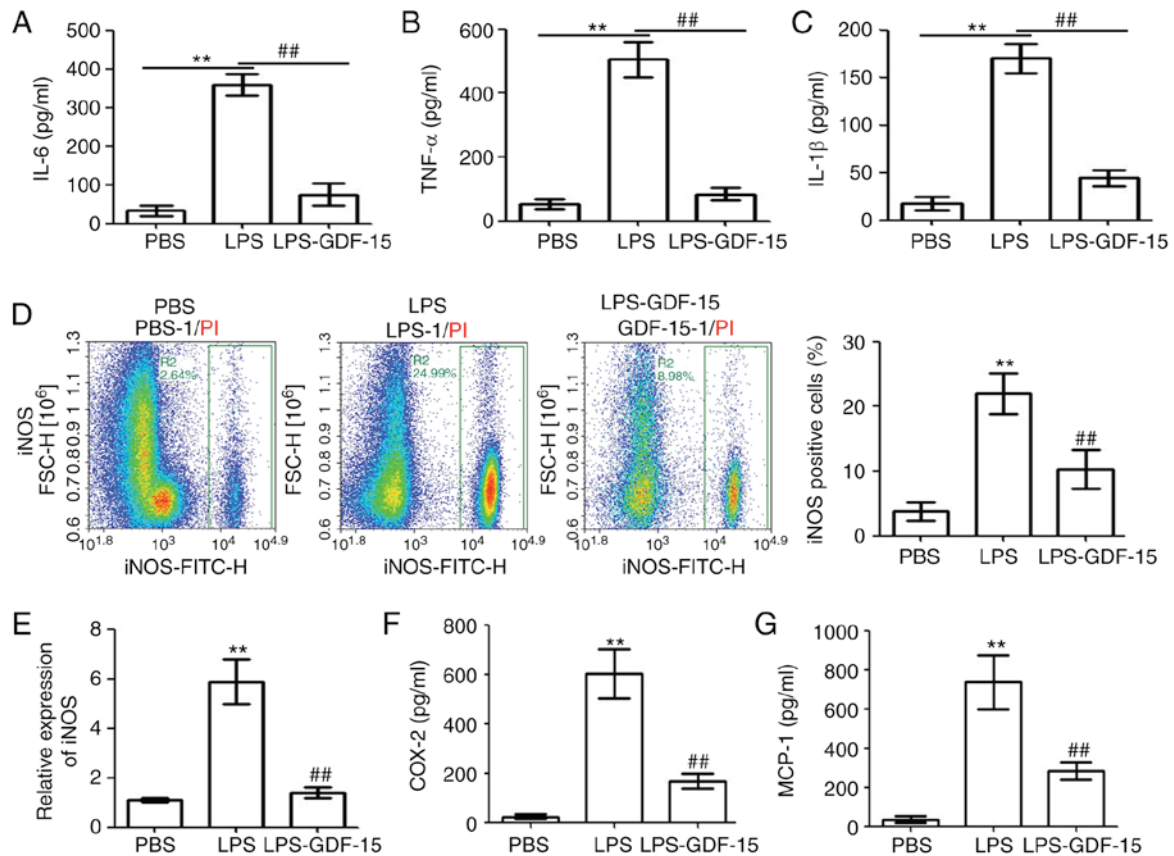


Figure 5. GDF-15 attenuates LPS-induced inflammation in Kupffer cells. (A) The levels of IL-6, (B) TNF- $\alpha$  and (C) IL-1 $\beta$  were evaluated in the supernatants of treated Kupffer cells by ELISA. (D) Flow cytometry analysis of iNOS-positive Kupffer cells following the indicated treatments. Representative plots and quantification are shown. (E) Relative mRNA expression levels of iNOS in Kupffer cells. (F) Levels of secreted COX-2 and (G) MCP-1 in the supernatants of Kupffer cells were evaluated by ELISA. \*\* $P < 0.01$  compared with PBS group; ## $P < 0.01$  compared with LPS group ( $n = 3$ ). GDF-15, growth differentiation factor-15; LPS, lipopolysaccharide; IL, interleukin; TNF, tumor necrosis factor; iNOS, inducible nitric oxide synthase; COX-2, cyclooxygenase-2; MCP-1, monocyte chemoattractant protein-1.

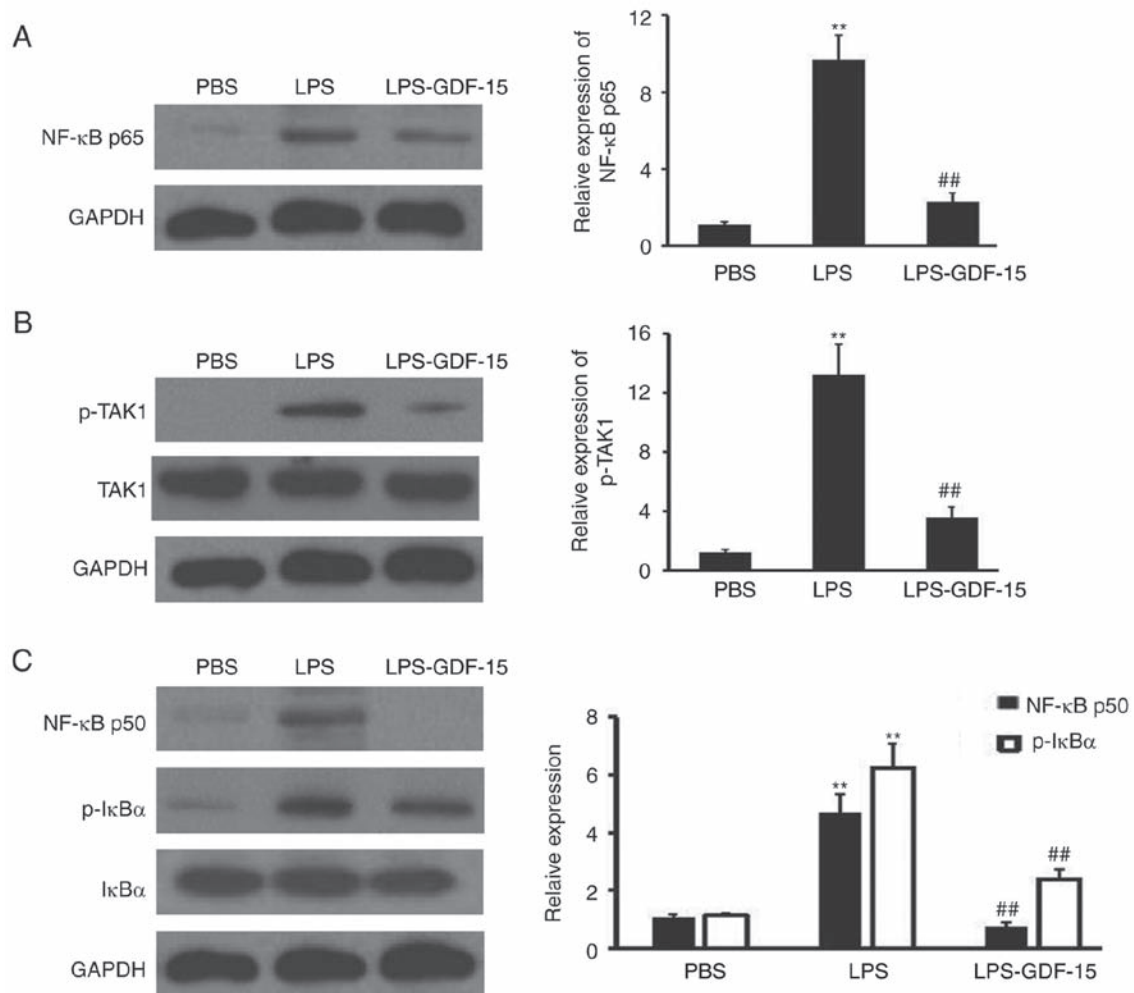


Figure 6. GDF-15 regulates the LPS-induced NF- $\kappa$ B pathway in Kupffer cells. Representative blots and quantification are shown from western blot analysis for the protein expression levels of (A) NF- $\kappa$ B p65, (B) p-TAK1 and TAK1, and (C) NF- $\kappa$ B p50, p-I $\kappa$ B $\alpha$  and I $\kappa$ B $\alpha$  in Kupffer cells. GAPDH was used as a loading control. \*\* $P < 0.01$  compared with PBS group; ## $P < 0.01$  compared with LPS group ( $n = 3$ ). GDF-15, growth differentiation factor-15; LPS, lipopolysaccharide; NF- $\kappa$ B, nuclear factor- $\kappa$ B; TAK1, transforming growth factor  $\beta$ -activated kinase 1; p-, phosphorylated; I $\kappa$ B $\alpha$ , NF- $\kappa$ B inhibitor  $\alpha$ .

I $\kappa$ B $\alpha$  was inhibited by GDF-15 treatment in Kupffer cells, compared with the LPS alone treatment group (Fig. 6C). Collectively, these results suggested that GDF-15 protected LPS-induced NF- $\kappa$ B pathway activation through regulating TAK1 phosphorylation in Kupffer cells.

## Discussion

The present study demonstrated that GDF-15 treatment reduced LPS/D-GalN-induced acute liver injury in mice, suggesting that GDF-15 was a preventive factor in the pathological process. The mechanism underlying the role of GDF-15 in preventing LPS/D-GalN-induced acute liver injury was further investigated. Lower levels of inflammatory cytokines and numbers of inflammatory macrophages (iNOS-positive) were measured in the GDF-15-treated group compared with the model group. Investigations of the molecular mechanism demonstrated that GDF-15 effectively protected against LPS-induced NF- $\kappa$ B pathway activation, by regulating TAK1 phosphorylation in Kupffer cells. In conclusion, GDF-15 reduced the activation of pro-inflammatory factors, and prevented LPS/D-GalN-induced liver injury, most likely by

disrupting TAK1 phosphorylation and consequently inhibiting the activation of the I $\kappa$ B $\alpha$ /NF- $\kappa$ B pathway in the liver.

GDF-15 is a divergent member of the human TGF- $\beta$  superfamily showing similarity to both classical TGF- $\beta$  isoforms and bone morphogenetic proteins (BMPs) (24). In healthy individuals, GDF-15 is strongly expressed in the placenta during pregnancy, and at low-to-moderate levels, in the brain, liver, breast, colon, and bone marrow (25). GDF-15 overexpression has been described in colorectal cancer and malignant glioma (25-27). Additionally, serum GDF-15 levels have been reported to correlate with heart failure (13), atrial fibrillation (12), atrial fibrosis (28), and cardiac injury (29). These previous findings possibly indicated that GDF-15 has heterogeneous functions in different diseases. Furthermore, a previous study indicated that decompensated liver cirrhosis patients had increased serum GDF-15 levels compared with patients with compensated liver cirrhosis and chronic hepatitis (30). Serum GDF-15 levels are significantly increased in critically ill patients, associated with sepsis, organ failure, and disease severity (31). However, the function of GDF-15 in sepsis remains unclear. The present study demonstrated that decreased LPS/GalN-induced acute liver injury was observed



in mice injected with GDF-15, accompanied with lower serum levels of AST and ALT. These findings suggested that GDF-15 is a preventive factor in this pathological process and a potential therapeutic agent for sepsis, although further research is required to examine the clinical importance of GDF-15 in sepsis in humans.

The inflammatory response following sepsis is important for the induction of liver injury (32,33). Thus, perturbation of the induction of the inflammatory response is a potential therapeutic strategy for liver injury (7,34,35). Upon stimulation of D-GalN-sensitized mice with LPS, the pro-inflammatory cytokines IL-1, IL-6 and TNF- $\alpha$  are secreted, inducing hepatocellular apoptosis, which has been identified as an early and possibly causal event in LPS/D-GalN-induced liver failure (36,37). In the present study, the inhibitory role of GDF-15 in LPS/D-GalN-induced inflammation was demonstrated, evidenced by the low levels of hepatic MDA, MPO, and pro-inflammatory cytokines in the mice treated with GDF-15. These findings were consistent with those of a previous study by Kim *et al*, reporting that transgenic mice expressing human NAG-1/GDF-15 have less white adipose tissue, which may be responsible for reduced inflammatory response to LPS (20).

Liver dysfunction following sepsis is an independent risk factor for multiple organ dysfunction and sepsis-induced death (32,38). Acting as a double-edged sword in sepsis, liver-mediated immune response is responsible for eliminating bacteria and toxins, although it also causes inflammation, immunosuppression, and organ damage (32,38). As key components of the hepatic innate immune system, Kupffer cells are postulated to have a central role in the response to LPS and as mediators of LPS-induced liver injury (39). Upon stimulation by LPS, Kupffer cells secrete pro-inflammatory molecules, including IL-1, IL-6, TNF- $\alpha$ , MCP-1 and COX-2 (40). In the present study, GDF-15 was demonstrated to significantly inhibit *in vivo* and *in vitro* inflammatory cytokine expression in murine Kupffer cells, accompanied with a decrease in numbers of pro-inflammatory macrophages. Further investigations of the molecular mechanism revealed that GDF-15 effectively protected against the activation of the NF- $\kappa$ B pathway, by regulating TAK1 phosphorylation in Kupffer cells. These results were consistent with those of a previous study, reporting that GDF-15 suppresses macrophage activity by inhibiting TAK1 signaling to NF- $\kappa$ B (23). However, there were some findings differing between the present study and this previous study, which demonstrated that GDF-15 did not inhibit LPS-induced cytokine expression in RAW264.7 cells or mouse Kupffer cells *in vitro* (20). It can be speculated that these discrepancies may result from the different treatment methods used.

In summary, the main findings of the present study, both *in vitro* and *in vivo*, demonstrated the preventive role and mechanism of GDF-15 against LPS/D-GalN-induced mortality, acute liver injury, and inflammatory response. Although further research is required to examine the clinical importance of the present findings, these results suggest a therapeutic potential for GDF-15 in sepsis treatment.

## Acknowledgements

Not applicable.

## Funding

The present study was supported by the Natural Science Foundation of China (grant no. 81560031).

## Availability of data and materials

The analyzed datasets generated during the study are available from the corresponding author on reasonable request.

## Authors' contributions

ML was involved in the acquisition of the data. KS, XWH and SMF were involved in the analysis and interpretation of the data. QYZ was involved in the conception and design of the present study and obtaining the funding.

## Ethics approval and consent to participate

The experimental protocols involving animals were approved by the Institutional Animal Use Committee of the Southern Medical University (Guangzhou, China).

## Patient consent for publication

Not applicable.

## Competing interests

The authors declare that they have no competing interests.

## References

1. Angus DC and van der Poll T: Severe sepsis and septic shock. *N Engl J Med* 369: 840-851, 2013.
2. Singer M, Deutschman CS, Seymour CW, Shankar-Hari M, Annane D, Bauer M, Bellomo R, Bernard GR, Chiche JD, Coopersmith CM, *et al*: The third international consensus definitions for sepsis and septic shock (Sepsis-3). *JAMA* 315: 801-810, 2016.
3. Cao Z and Robinson RA: The role of proteomics in understanding biological mechanisms of sepsis. *Proteomics Clin Appl* 8: 35-52, 2014.
4. Hamers L, Kox M and Pickkers P: Sepsis-induced immunoparalysis: Mechanisms, markers, and treatment options. *Minerva Anesthesiol* 81: 426-439, 2015.
5. Chun K, Syndergaard C, Damas C, Trubey R, Mukindaraj A, Qian S, Jin X, Breslow S and Niemz A: Sepsis pathogen identification. *J Lab Autom* 20: 539-561, 2015.
6. Tacke F and Zimmermann HW: Macrophage heterogeneity in liver injury and fibrosis. *J Hepatol* 60: 1090-1096, 2014.
7. Ge X, Feng Z, Xu T, Wu B, Chen H, Xu F, Fu L, Shan X, Dai Y, Zhang Y and Liang G: A novel imidazopyridine derivative, X22, attenuates sepsis-induced lung and liver injury by inhibiting the inflammatory response *in vitro* and *in vivo*. *Drug Des Devel Ther* 10: 1947-1959, 2016.
8. Huang C, Wang J, Chen Z, Wang Y and Zhang W: 2-Phenylethanesulfonamide prevents induction of pro-inflammatory factors and attenuates LPS-induced liver injury by targeting NHE1-Hsp70 complex in mice. *PLoS One* 8: e67582, 2013.
9. Scott MJ, Liu S, Shapiro RA, Vodovotz Y and Billiar TR: Endotoxin uptake in mouse liver is blocked by endotoxin pretreatment through a suppressor of cytokine signaling-1-dependent mechanism. *Hepatology* 49: 1695-1708, 2009.
10. Wang JB, Wang HT, Li LP, Yan YC, Wang W, Liu JY, Zhao YT, Gao WS and Zhang MX: Development of a rat model of D-galactosamine/lipopolysaccharide induced hepatorenal syndrome. *World J Gastroenterol* 21: 9927-9935, 2015.



11. Unsicker K, Spittau B and Krieglstein K: The multiple facets of the TGF- $\beta$  family cytokine growth/differentiation factor-15/macrophage inhibitory cytokine-1. *Cytokine Growth Factor Rev* 24: 373-384, 2013.
12. Hijazi Z, Oldgren J, Andersson U, Connolly SJ, Eikelboom JW, Ezekowitz MD, Reilly PA, Yusuf S, Siegbahn A and Wallentin L: Growth-differentiation factor 15 (GDF-15) in patients admitted for acute heart failure: Results from the RELAX-AHF study. *Eur J Heart Fail* 17: 1133-1143, 2015.
13. Cotter G, Voors AA, Prescott MF, Felker GM, Filippatos G, Greenberg BH, Pang PS, Ponikowski P, Milo O, Hua TA, *et al*: Growth differentiation factor 15 (GDF-15) in patients admitted for acute heart failure: Results from the RELAX-AHF study. *Eur J Heart Fail* 17: 1133-1143, 2015.
14. Abulizi P, Loganathan N, Zhao D, Mele T, Zhang Y, Zwiep T, Liu K and Zheng X: Growth differentiation factor-15 deficiency augments inflammatory response and exacerbates septic heart and renal injury induced by lipopolysaccharide. *Sci Rep* 7: 1037, 2017.
15. Yan D, Liu HL, Yu ZJ, Huang YH, Gao D, Hao H, Liao SS, Xu FY and Zhou XY: BML-111 protected LPS/D-GalN-induced acute liver injury in rats. *Int J Mol Sci* 17: pii: E1114, 2016.
16. Dai L, Cui X, Zhang X, Cheng L, Liu Y, Yang Y, Fan P, Wang Q, Lin Y, Zhang J, *et al*: SARI inhibits angiogenesis and tumour growth of human colon cancer through directly targeting ceruloplasmin. *Nat Commun* 7: 11996, 2016.
17. t'Hart BA, Vervoordeldonk M, Heeney JL and Tak PP: Gene therapy in nonhuman primate models of human autoimmune disease. *Gene Ther* 10: 890-901, 2003.
18. Mikic AN, Brkic S, Maric D, Sekulic B, Cetkovic A and Mitic G: Thiobarbituric acid reactive substances as marker of oxidative stress in pregnancies with pre-eclampsia. *Med Pregl* 64: 377-380, 2011.
19. Liu MW, Liu R, Wu HY, Zhang W, Xia J, Dong MN, Yu W, Wang Q, Xie FM, Wang R, *et al*: Protective effect of Xuebijing injection on D-galactosamine- and lipopolysaccharide-induced acute liver injury in rats through the regulation of p38 MAPK, MMP-9 and HO-1 expression by increasing TIPE2 expression. *Int J Mol Med* 38: 1419-1432, 2016.
20. Kim JM, Kosak JP, Kim JK, Kissling G, Germolec DR, Zeldin DC, Bradbury JA, Baek SJ and Eling TE: NAG-1/GDF15 transgenic mouse has less white adipose tissue and a reduced inflammatory response. *Mediators Inflamm* 2013: 641851, 2013.
21. Schneider CA, Rasband WS and Eliceiri KW: NIH Image to ImageJ: 25 years of image analysis. *Nat Methods* 9: 671-675, 2012.
22. Livak KJ and Schmittgen TD: Analysis of relative gene expression data using real-time quantitative PCR and the  $2^{-\Delta\Delta CT}$  method. *Methods* 25: 402-408, 2001.
23. Ratnam NM, Peterson JM, Talbert EE, Ladner KJ, Rajasekera PV, Schmidt CR, Dillhoff ME, Swanson BJ, Haverick E, Kladney RD, *et al*: NF-kappaB regulates GDF-15 to suppress macrophage surveillance during early tumor development. *J Clin Invest* 127: 3796-3809, 2017.
24. Bootcov MR, Bauskin AR, Valenzuela SM, Moore AG, Bansal M, He XY, Zhang HP, Donnellan M, Mahler S, Pryor K, *et al*: MIC-1, a novel macrophage inhibitory cytokine, is a divergent member of the TGF-beta superfamily. *Proc Natl Acad Sci USA* 94: 11514-11519, 1997.
25. Liu DD and Mei YA: Effects of growth differentiation factor-15 (GDF-15) on neurological systems, cardiovascular diseases, and cancer progression. *Sheng Li Xue Bao* 69: 109-121, 2017 (In Chinese).
26. Sandor N, Schilling-Toth B, Kis E, Benedek A, Lumniczky K, Safrany G and Hegyesi H: Growth differentiation factor-15 (GDF-15) is a potential marker of radiation response and radiation sensitivity. *Mutat Res Genet Toxicol Environ Mutagen* 793: 142-149, 2015.
27. Unal B, Alan S, Bassorgun CI, Karakas AA, Elpek GO and Ciftcioglu MA: The divergent roles of growth differentiation factor-15 (GDF-15) in benign and malignant skin pathologies. *Arch Dermatol Res* 307: 551-557, 2015.
28. Zhou YM, Li MJ, Zhou YL, Ma LL and Yi X: Growth differentiation factor-15 (GDF-15), novel biomarker for assessing atrial fibrosis in patients with atrial fibrillation and rheumatic heart disease. *Int J Clin Exp Med* 8: 21201-21207, 2015.
29. Kahli A, Guenancia C, Zeller M, Grosjean S, Stamboul K, Rochette L, Girard C and Vergely C: Growth differentiation factor-15 (GDF-15) levels are associated with cardiac and renal injury in patients undergoing coronary artery bypass grafting with cardiopulmonary bypass. *PLoS One* 9: e105759, 2014.
30. Lee ES, Kim SH, Kim HJ, Kim KH, Lee BS and Ku BJ: Growth differentiation factor 15 predicts chronic liver disease severity. *Gut Liver* 11: 276-282, 2017.
31. Buendgens L, Yagmur E, Bruensing J, Herbers U, Baack C, Trautwein C, Koch A and Tacke F: Growth differentiation factor-15 is a predictor of mortality in critically ill patients with sepsis. *Dis Markers* 5271203: 2017, 2017.
32. Hoque R, Farooq A and Mehal WZ: Sterile inflammation in the liver and pancreas. *J Gastroenterol Hepatol* 28: (Suppl 1): S61-S67, 2013.
33. Mehal WZ: The inflammasome in liver injury and non-alcoholic fatty liver disease. *Dig Dis* 32: 507-515, 2014.
34. Ambade A, Catalano D, Lim A and Mandrekar P: Inhibition of heat shock protein (molecular weight 90 kDa) attenuates proinflammatory cytokines and prevents lipopolysaccharide-induced liver injury in mice. *Hepatology* 55: 1585-1595, 2012.
35. Baranova IN, Souza AC, Bocharov AV, Vishnyakova TG, Hu X, Vaisman BL, Amar MJ, Chen Z, Kost Y, Remaley AT, *et al*: Human SR-BI and SR-BII potentiate lipopolysaccharide-induced inflammation and acute liver and kidney injury in mice 196: 3135-3147, 2016.
36. Liao WQ, Qi YL, Wang L, Dong XM, Xu T, Ding CD, Liu R, Liang WC, Lu LT, Li H, *et al*: Recql5 protects against lipopolysaccharide/D-galactosamine-induced liver injury in mice. *J Immunol* 21: 10375-10384, 2015.
37. Zhang J, Xu L, Zhang L, Ying Z, Su W and Wang T: Curcumin attenuates D-galactosamine/lipopolysaccharide-induced liver injury and mitochondrial dysfunction in mice. *J Nutr* 144: 1211-1218, 2014.
38. Yan J, Li S and Li S: The role of the liver in sepsis. *Int Rev Immunol* 33: 498-510, 2014.
39. Dixon LJ, Barnes M, Tang H, Pritchard MT and Nagy LE: Kupffer cells in the liver. *Compr Physiol* 3: 785-797, 2013.
40. Tsutsui H and Nishiguchi S: Importance of Kupffer cells in the development of acute liver injuries in mice. *Int J Mol Sci* 15: 7711-7730, 2014.